David B. Marshall[1] *and Brian R. Lawn*[2]

Authorized Reprint from Special Technical Publication 889

Indentation of Brittle Materials

REFERENCE: Marshall, D. B. and Lawn, B. R., **"Indentation of Brittle Materials,"** *Microindentation Techniques in Materials Science and Engineering, ASTM STP 889*, P. J. Blau and B. R. Lawn, Eds., American Society for Testing and Materials, Philadelphia, 1986, pp. 26–46.

ABSTRACT: The use of indentation testing as a method for investigating the deformation and fracture properties of intrinsically brittle materials, glasses, and ceramics is examined. It is argued that the traditional plasticity models of hardness phenomena can be deficient in some important respects, notably in the underlying assumptions of homogeneity and volume conservation. The penetrating indenter is accommodated by an intermittent "shear faulting" mode, plus (to a greater or lesser extent, depending on the material) some structural compaction or expansion. These faults provide the sources for initiation of the indentation cracks. Once generated, the cracks can grow under the action of subsequent external tensile stresses, thereby taking the specimen to failure.

In this presentation the mechanical basis for describing these phenomena will be outlined, with particular emphasis on the interrelations between hardness and other characteristic material parameters, such as elastic modulus and fracture toughness. Procedures for quantitative determination of these parameters will be discussed. Extension of the procedures to the measurement of surface residual stresses in brittle materials will be made to illustrate the power of the indentation method as an analytical tool for materials evaluation.

KEY WORDS: Microindentation hardness testing, brittleness, cracks, elastic recovery, fracture mechanics, indentation, residual stress, shear faults, toughness

Indentation methods are now widely used to study the mechanical properties of glasses and ceramics. The contact of a sharp diamond point with even the most brittle surface causes some irreversible deformation and leaves a residual impression from which a measure of the hardness can be obtained. There is also evidence (for example, from the recovery of the indentations during unloading) that the elasticity of the test material plays a far from insignificant role in the contact process. But the overwhelmingly distinctive fea-

[1]Manager, Structural Ceramics Department, Rockwell International Science Center, Thousand Oaks, CA 91360.

[2]Physicist, Center for Materials Science, National Bureau of Standards, Gaithersburg, MD 20899.

ture of the indentation patterns in this class of materials is the almost invariable appearance of so-called radial cracks emanating from the impression corners. It becomes clear that the potential exists for obtaining quantitative information on fracture as well as deformation properties from a simple hardness testing facility.

In addition to its simplicity, indentation testing has several attractions as a tool for characterizing the mechanical response of brittle materials. The geometry and size of the crack patterns can be accurately controlled and the location of the contact site predetermined. We thereby have a well-defined system for analysis in terms of "fracture mechanics" methodology [*1*,*2*]. Microscopic examination of the indentation area, both during and after the actual contact process, provides valuable information on the fundamental mechanisms of deformation and fracture. Indentation damage usefully simulates individual events in a range of cumulative surface removal processes, such as abrasive wear and machining, and accordingly serves as a base for setting up detailed models of these processes. Radial cracks can be used as strength-controlling "flaws" in the failure testing of ceramics, thus allowing the determination of fracture toughness parameters with high accuracy. Experiments of this kind have provided a unique link between the mechanical response of brittle materials at the microscopic level and the more traditional approach of macroscopic fracture testing adopted by engineering researchers.

The primary aim of this paper is to survey areas of research in which indentations have been used to determine the mechanical properties of glasses and ceramics. Various aspects of this topic have been discussed at length in other review articles [*2*–*7*], so our coverage here is not intended to be in any way exhaustive. To begin, some basic observations of the nature of sharp-indenter damage and how these observations fit into a general fracture mechanics formalism will be presented. Comment will be made on the underlying structural processes which accommodate the indentation deformation and the associated crack configurations. Then two major practical applications will be described: the measurement of brittle fracture parameters and the evaluation of surface stresses. Our emphasis here is on physical principles rather than mathematical details, although we shall include some of the more important equations to demonstrate the power of the fracture mechanics approach.

Characteristics of Indentation Damage in Brittle Materials

General Observations

As with metals, the contact of a glass or ceramic surface with a sharp, fixed-profile indenter leaves a residual impression, indicating some form of irreversible deformation. Casual observation of the contact site shows nothing unusual about the appearance of the depressed material; the imprint of the

indenter is well defined, and the surface regions within the imprint appear characteristically smooth. At first sight, therefore, one might feel justified in adopting the same, traditional plasticity models used to describe the deformation response in ductile materials [*8,9*]. And, in fact, this approach has met with a certain degree of success in the description of the hardness properties of brittle surfaces [*10*]. The picture most commonly conjured up is that of an "expanding cavity," in which the volume of the impression is accommodated by a net radial flow of material, resulting in an approximately hemispherical plastic zone surrounded by a confining elastic matrix. A distinctive feature of such radial flow models is a predicted absence of "pileup" around the indentation, a prediction borne out (at least in the harder ceramics and glasses) by experimental observation [*10*]. It is implicit in all continuum-based plasticity models of this kind that the deformation processes are volume conserving (as characterized by a well-defined yield stress), a consequence of which is that a state of residual stress must exist around the indentation site [*11*].

Closer inspection of the deformation regions beneath the contact area reveals some important departures from the idealized picture just presented. First, the deformation processes are by no means uniformly distributed within the plastic zone but are manifested (at least in part) as a cumulation of discrete shear events. These events are akin to the dislocation slip processes which occur on preferential glide planes in softer materials, but can differ in two important respects: (1) they occur at stress levels close to the theoretical shear strength of the structure in the more covalent materials, and (2) the shear surfaces are not necessarily crystallographic (similar shear events are observed in glassy and in crystalline materials) but are determined more by stress trajectory patterns [*12*]. One therefore has to be extremely cautious before using classical dislocation concepts to describe the flow properties of solids with intrinsically rigid bonding.

A second departure from ideal behavior is apparent in certain materials which show a greater tendency toward deformation in hydrostatic stress than in shear. Fused silica, for instance, undergoes structural densification when subjected to confining pressures [*13*]. (The term *anomalous* has been used to describe glasses of this kind.) Many crystalline solids undergo pressure-induced phase transformations, which may be either expansive (for example, in zirconia composites) or compactive. Compaction modes can accommodate the volume of the impression with relatively little stress mismatch at the deformation zone boundary [*14*].

A clear illustration of such effects is given in Fig. 1. The micrographs are of Vickers indentations in soda lime and fused silica glasses [*15*]. The section views are obtained by indenting across a preexisting hairline fissure and then running this fissure through the specimen. Well-defined shear faults are distinguishable in the cross-sectional view in the soda lime glass. It is envisaged

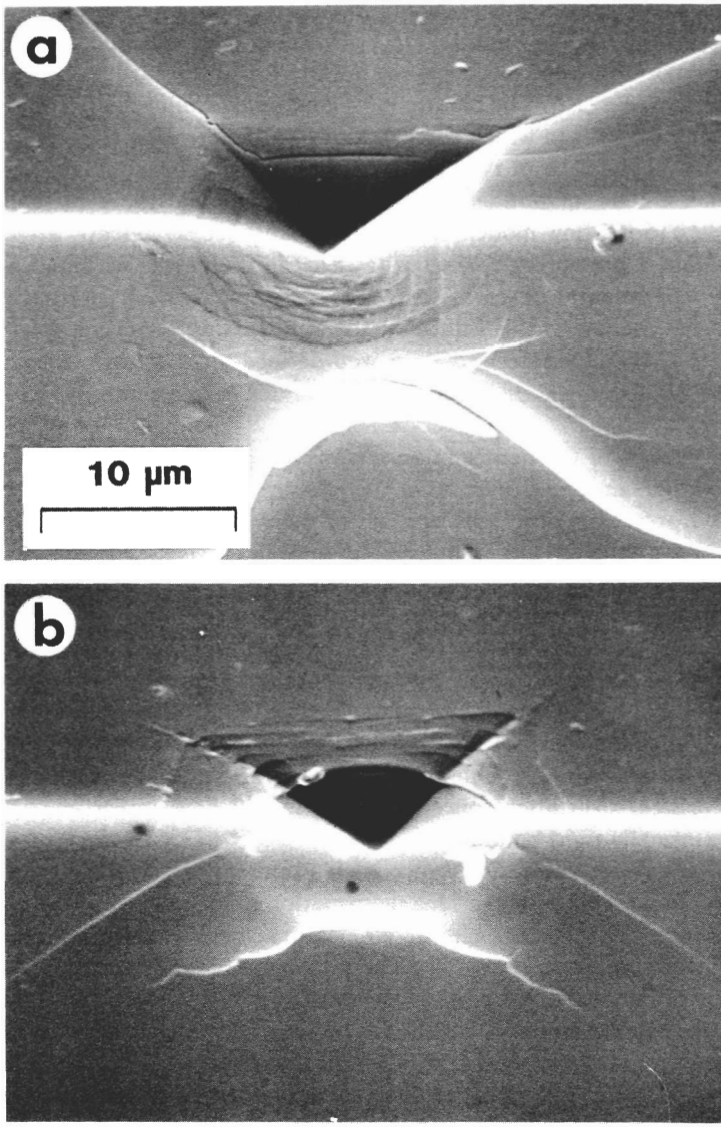

FIG. 1—*Scanning electron micrographs of Vickers indentations in* (a) *soda lime and* (b) *fused silica glasses, showing half-surface and section views.*

that these faults are produced as catastrophic slip failures as a result of the punching action of the penetrating indenter. Once such a failure occurs, the local stress intensity will be somewhat relieved, so that further penetration is needed to produce the next fault; this explains the periodic nature of the pattern. In the fused silica, the surface pattern of the slip traces is not dissimilar, but the faults do not penetrate deeply into the subsurface regions. In this latter glass, structural compaction absorbs a greater proportion of the indentation energy.

As mentioned previously, an indicator of brittleness in an indentation experiment is the appearance of radial cracks at the corners of the residual impression. Figure 2 illustrates schematically the characteristic fracture pattern for a Vickers indentation. The radial cracks are oriented normal to the specimen surface, on so-called median planes coincident with the impression diagonals, and have a half-penny configuration with their centers at the original contact point. A second set of cracks, called lateral cracks, extends from near the base of the deformation zone into a subsurface saucerlike configuration. A general discussion of the geometrical features of these crack patterns is to be found in Refs *2* and *16*.

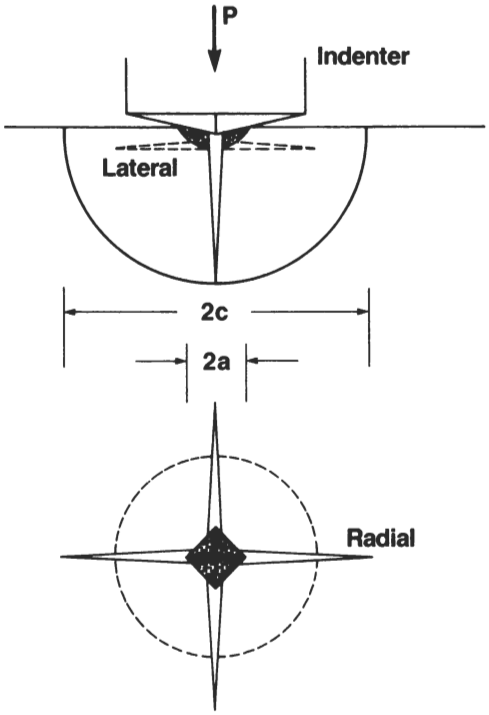

FIG. 2—*Indentation fracture pattern, depicted here for Vickers geometry.*

Let us now consider the nature of the processes responsible for *initiating* and *propagating* the cracks. From close observation of the indentation sites, for example, as in Fig. 1, it becomes clear that the shear events referred to earlier are critically important in acting as embryonic nuclei for crack formation [*12,15-17*]. (Cracks can be thus initiated in the most perfect of surfaces, such as freshly drawn optical fibers, which are free of preexisting defects down to molecular dimensions [*18*].) There is a threshold indent size, typically ≈ 10 μm, below which crack initiation does not occur, although this threshold is subject to considerable variation, depending on such things as the duration of contact and the test environment [*17*]. Once initiated, the cracks "pop in" abruptly, to a characteristic length ≈ 100 μm, at which stage they are considered to be fully propagating. It is observed that most of the crack development occurs not on loading, but on *un*loading, the indenter, indicating that it is the *ir*reversible component of the contact stress field which provides the dominant driving force for fracture. The sequence of micrographs of crack evolution during Vickers indentation in soda lime glass in Fig. 3 illustrates the point [*19*]. Note also the appearance of the stress birefringence in the final frame of this sequence; glass is not optically active, so the persistence of the "Maltese cross" in this frame confirms the existence of a substantial residual stress intensity.

An even more dramatic indication of residual stress effects in the fracture evolution is manifest in postindentation observations. At loads above threshold, the popped-in cracks are often seen to continue propagating well after completion of the contact. Below threshold, delayed pop-in can occur. These phenomena are attributable to the time-dependent enhancement of crack development in the presence of moisture, as alluded to in the previous paragraph.

Mechanics

Evaluation of the indentation cracking properties of brittle materials requires a knowledge of the underlying fracture mechanics. The starting point for the requisite formulation is the characterization of the elastic-plastic stress field, with particular focus on the residual component of this field. Unfortunately, this formulation can be a formidable task, even for the idealization of a perfectly homogeneous, continuous solid. The difficulty is especially pronounced in the modeling of crack initiation, for there one is concerned with the complex details of the contact near field [*2*]. Things are not so bad once the crack is in its fully propagating stage, in which the far field may be regarded in terms of simple "point" force solutions. Within these limitations, working equations defining the scale of the indentation damage as a function of contact load can be developed from first principles.

Let us begin with a consideration of the manner with which the indenter load, P, varies with the penetration, z, during a contact cycle. Experimen-

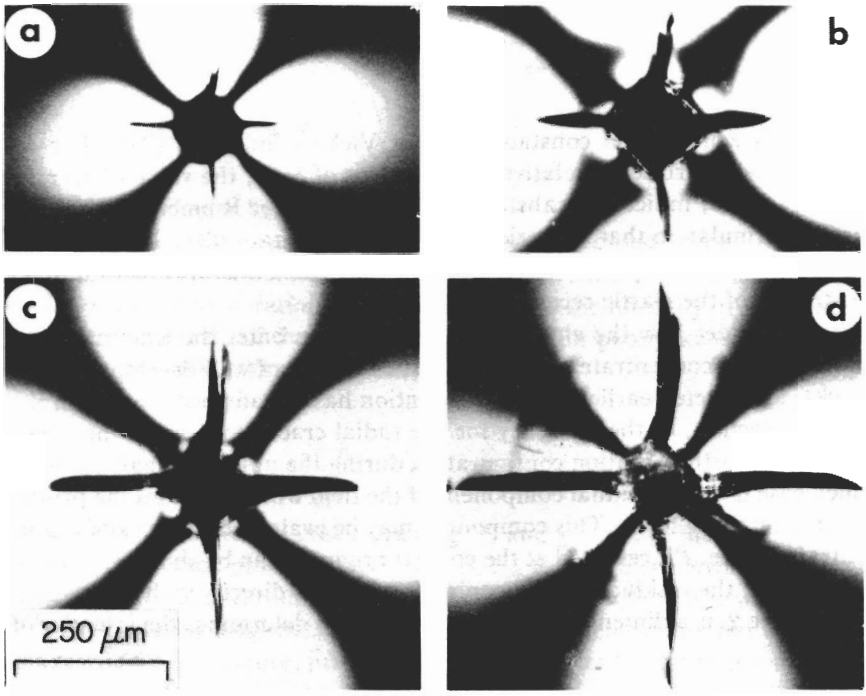

FIG. 3—In situ *observations of Vickers indentation in soda lime glass, viewed from below during the loading cycle. The sequence shows the* (a) *half-loaded,* (b) *fully loaded,* (c) *half-unloaded, and* (d) *fully unloaded stages. Note the development of radial cracks to completion during the unloading half-cycle. Polarized light reveals strong stress birefringence.*

tally, the function $P(z)$ is found to have the form shown in Fig. 4. During the loading half-cycle, the contact pressure ($\propto P/a^2$, where a is a characteristic impression dimension) remains constant (at least in the region where geometrical similarity prevails). This pressure, by definition, determines the hardness. The deformation has both elastic and inelastic components at this stage. On unloading, the deformation is entirely elastic (*re*loading simply reproduces the unloading curve). Hence, the contact pressure in the unload region is determined by Young's modulus, E. We may write the functional relations for the two half-cycles in the form [*20*]

$$P \propto Hz^2 \qquad \text{(load)} \tag{1a}$$

$$P \propto E(z^2 - z_r^2) \qquad \text{(unload)} \tag{1b}$$

where due allowance is made in Eq 1*b* for the existence of a residual impression depth, z_r. The requirement for compatibility of these two equations at the maximum penetration, z_m, yields the relation

$$\left(\frac{z_r}{z_m}\right)^2 = 1 - \frac{\eta H}{E} \tag{2}$$

where η is a numerical constant (≈ 6 for Vickers indenters [*20*]). For ceramics, characterized by relatively high values of H/E, the value of z_r/z_m is typically ≈ 0.5, indicating substantial elastic recovery. It emerges from this kind of formulation that the ratio H/E has an important place in the specification of the elastic-plastic field. The same conclusion is drawn from other treatments of the elastic recovery problem [*21*,*22*].

Now consider how the elastic-plastic parameters enter the fracture problem. We shall concentrate on the simplest case, that of well-developed radial cracks, as depicted earlier in Fig. 2. Mention has already been made, in the previous section, of the tendency for the radial cracks to develop into their immediate postindentation configuration during the unloading half-cycle, in which case it is the residual component of the field which provides the principal crack driving force. This component may be evaluated in terms of a concentrated force, P_r, centered at the contact origin. It can be shown that $P_r = \chi_r P$, that is, the residual crack-opening force scales directly with the contact load, where χ_r is a dimensionless parameter which determines the intensity of

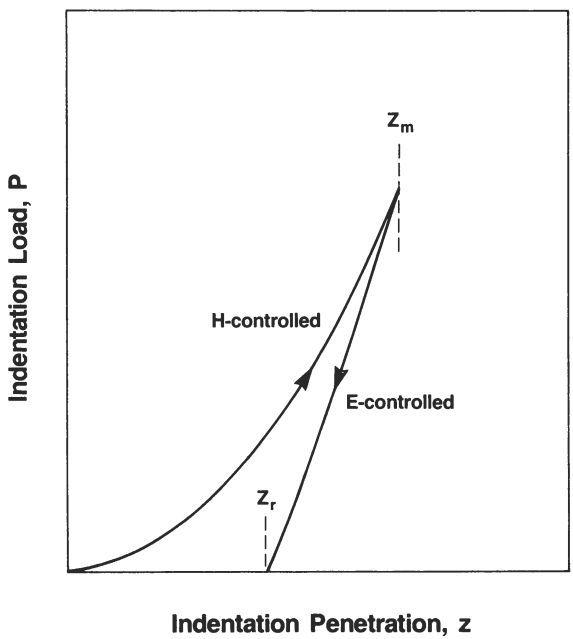

FIG. 4—*Load-displacement response for sharp indenters.*

the field [*19*]. For an ideal elastic-plastic material in which the irreversible deformation is volume conserving, analysis gives [*23*]

$$\chi_r \propto \left(\frac{E}{H}\right)^{1/2} (\cot \phi)^{2/3} \tag{3}$$

where ϕ is the indenter half-angle.

The next step is to incorporate the center-load force into an appropriate fracture mechanics formulation. This is most conveniently done using the *stress intensity factor* notation, K, which expresses the intensity of the field concentrated at the tip of the extending crack [*1*]. For pennylike cracks, the stress intensity factor takes on the form [*19*]

$$K_r = \frac{\chi P}{c^{3/2}} \tag{4}$$

where c is the characteristic crack size (Fig. 2) and $\chi \propto \chi_r$. In the absence of time-dependent crack growth effects, that is, for tests in inert environments, the condition for equilibrium extension is expressible as $K = K_c$, where K_c defines the material toughness. This toughness parameter quantifies the intrinsic resistance to fracture, just as hardness quantifies the resistance to deformation. Insertion of this requirement into Eq 4 then gives the equilibrium crack length

$$c_0 = \left(\frac{\chi P}{K_c}\right)^{2/3} \tag{5}$$

at completion of indentation.

An analogous expression to that in Eq 5 can be obtained for lateral cracks, although the analysis is somewhat more complicated because of the relatively high compliance of the thin layer of material which overlays the crack plane [*24*].

A configuration of special interest is that of an indented specimen subsequently subjected to an externally applied tensile stress, for example, as in a bend test. The radial cracks can then be emplaced so as to be normal to the tensile direction, and thereby act as strength-controlling flaws. A unique feature of such a "controlled-flaw" test is the facility to predetermine the failure site, so that the crack response can be observed directly throughout its evolution to failure [*25*]. Such observations reveal a new kind of flaw behavior. Whereas the earlier, classic study by Griffith (see Ref *1*) suggested that the size of flaws should remain stationary up to the critical load for failure, at which point the equilibrium is unstable, it has been observed in the indenta-

tion experiments that a significant amount of precursor extension precedes the instability configuration. This stabilization of the crack system is attributable to the residual driving force, K_r, in Eq 4, which augments the applied loading. It should be noted that whereas the external loading term, K_a, is always an increasing function of crack size [*1*], K_r is a decreasing function. Formally, superposition of K_a and K_r gives, at equilibrium [*25*]

$$K = \psi\sigma_a c^{1/2} + \frac{\chi P}{c^{3/2}} = K_c \tag{6}$$

where σ_a is the applied tensile stress, and ψ is a crack geometry constant (of the order unity). The condition for *unstable* equilibrium is that K should have a minimum value in Eq 6. Putting $dK/dc = 0$, accordingly determines the critical configuration

$$\sigma_m = \frac{3K_c}{4\psi c_m^{1/2}} \tag{7a}$$

$$c_m = \left(\frac{4\chi P}{K_c}\right)^{2/3} \tag{7b}$$

at failure. Note that c_m in Eq 7*b* is $4^{2/3} = 2.52$ times c_0 in Eq 5, indicating that the stage of precursor crack growth is by no means insignificant.

The fracture mechanics formulations to this point are contingent on the threshold load being exceeded. If this threshold is *not* exceeded, we are faced with the considerably more complex problem of crack initiation, in which the corresponding relations for crack instability involve detailed analysis of the near-field conditions. Phenomenological treatments of the instability condition for spontaneous radial crack pop-in from an incipient nucleus, based on the hypothesis that the *intensity* of the indentation stress field should remain invariant (since it scales directly with the hardness) while the *spatial extent* should scale directly with the indent size, a, predict a critical threshold condition [*26,27*]

$$a_c = \mu\left(\frac{K_c}{H}\right)^2 \tag{8}$$

where $\mu \propto E/H$. Hence, the initiation mechanics reflect an inherent size effect. This size effect relates to the fact that, while the resistance to deformation, H, has the units of stress, the fracture resistance, K_c, has the units of stress multiplied by dimension to the one half power (as is evident from Eq 6).

Measurement of Material Properties

Elastic Recovery

Measurements of the elastic recovery at hardness indentations are of interest for the light they shed on the partition of input deformation energy into reversible and irreversible components and for their characterization of the elastic-plastic field in the ensuing fracture mechanics formalism. (They can also be used to evaluate Young's modulus at a microscopic level.) The parameter of interest here is the ratio of hardness to modulus, H/E. One way of measuring this parameter is to monitor the load-penetration function, $P(z)$, and to make use of Eqs 1 and 2 [*20*] or some equivalent analytical expressions [*22*]. (The theme of load-penetration characteristics to determine indentation response is, incidentally, a recurring one in this volume.) Unfortunately, the apparatus needed to measure indentation displacements is not yet a standard accessory on most hardness testing facilities, so quantitative studies of elastic recovery have not occupied a prominent place in the deformation evaluation literature.

However, one way in which a measure of the recovery can be obtained without recourse to special equipment is to observe the relative contraction of the surface diagonals of Knoop impressions [*21*]. Whereas the long diagonal turns out to be relatively insensitive to "springback" effects, the short diagonal does not. (The analogy with the age-old problem of trying to break an egg by pressing along the longitudinal axis is instructive here.) Analysis gives

$$\frac{b'}{a'} = \frac{b}{a} - \frac{\alpha H}{E} \tag{9}$$

where $b/a = 1/7.11$ is the *nominal* ratio of short to long half-diagonal, b'/a' is the corresponding value after recovery, and α is a dimensionless constant (≈ 0.45 [*21*]). Hence, materials with relatively rigid structures, that is, high H/E, are likely to show greater lateral recovery. This is evident in Fig. 5, which contrasts Knoop indentations of similar length in two extreme materials, zinc sulfide (ZnS) ($H/E = 0.02$) and soda lime glass ($H/E = 0.09$) [*21*]. Figure 6 shows the validity of Eq 9 for a wider range of materials [*21*].

Fracture Toughness

Perhaps the most widespread use of indentation testing in the context of brittle materials is the evaluation of material toughness. In this application, one seeks to relate the fracture resistance to the scale of the crack pattern. It is perhaps ironical that the earlier hardness testing fraternity tried to avoid cracking like the plague, whereas now the indentation method has become

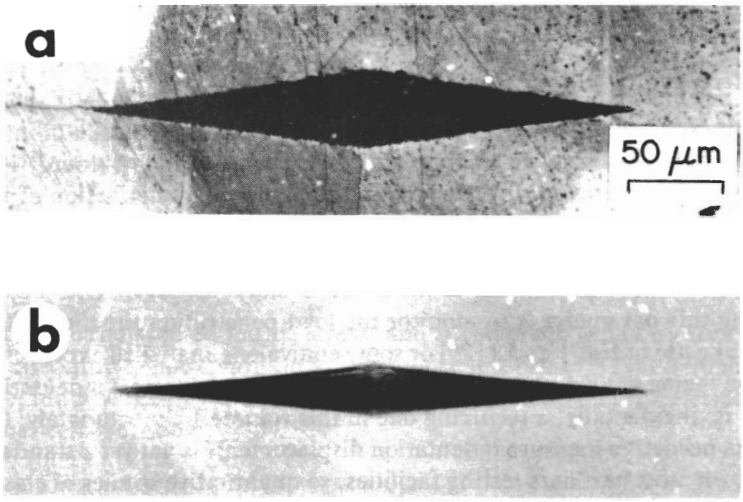

FIG. 5—*Knoop indentations in* (a) *polycrystalline zinc sulfide and* (b) *soda lime glass. Note the relatively strong elastic recovery of the short diagonal in the latter material.*

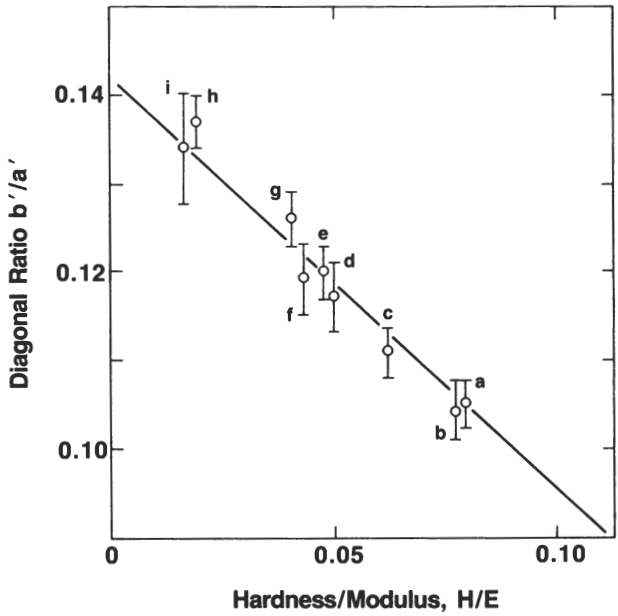

FIG. 6—*Plot of the short-to-long-diagonal ratio,* b′/a′, *from Knoop indentation measurements against* H/E *for selected materials:* (a) *soda lime glass,* (b) *glass ceramic,* (c) *silicon nitride,* (d) *alumina,* (e) *zirconia,* (f) *magnesium fluoride,* (g) *steel,* (h) *zinc sulfide, and* (i) *zinc oxide.*

the most commonly used of all toughness measurement techniques in glass and ceramics. Here we describe three variants of the indentation procedure.

1. The first and most straightforward approach involves relating toughness, K_c, directly to postindentation crack size, c_0. Palmqvist [*28*] was the first to recognize the potential for such a relationship, but his treatment was purely empirical. We now have, through Eqs 3 and 5, the means for deriving an appropriate expression from first principles

$$K_c = \xi\left(\frac{E}{H}\right)^{1/2} \frac{P}{c_0^{3/2}} \tag{10}$$

where ξ is a dimensionless constant [*29*]. Thus, we have, in principle, a simple means of determining K_c, with the capacity for making many measurements on a single surface.

2. The second method makes use of the special crack response implicit in the derivation of the instability relations in Eq 7. The test procedure involves emplacing a controlled indentation flaw in the prospective tensile face of a bend bar and then measuring the strength of the bar in an inert environment. Eliminating c_m from Eqs 7*a* and 7*b*, and combining with Eq 3, we obtain

$$K_c = \eta\left(\frac{E}{H}\right)^{1/8} (\sigma_m P^{1/3})^{3/4} \tag{11}$$

where η is another dimensionless constant [*30*]. Note that strength replaces crack size as a test variable in this formulation, a distinct advantage in materials in which direct crack observations are difficult (as is true with many ceramics). However, only one test result is obtained per specimen.

3. The third method is a hybrid of the first two in that it involves measurement of *both* crack size and strength. The appropriate toughness relation derives directly from Eq 7*a* [*31*]

$$K_c = \left(\frac{4\psi}{3}\right)\sigma_m c_m^{1/2} \tag{12}$$

Although the measurement requirements are clearly more stringent, the method has the advantage of circumventing knowledge of the E/H parameter. It will be recalled that this parameter is determined from Eq 3, the basis of which is volume conservation in the deformation process. The specific advantage of Eq 12 is that it contains no implicit assumption at all concerning the mode of deformation. Experimentally, c_m can be conveniently determined by introducing *several* nominally identical indentations within the tensile test span of the bend specimen; failure occurs from just one of the indentations,

leaving "survivors" for measurement of the *near*-critical crack lengths [*31*,*32*].

The results of measurements on selected glasses and ceramics are shown in Fig. 7 for each of these three variant methods [*29–31*]. Each plot is reasonably well represented by a linear fit, although the lines do not pass through the

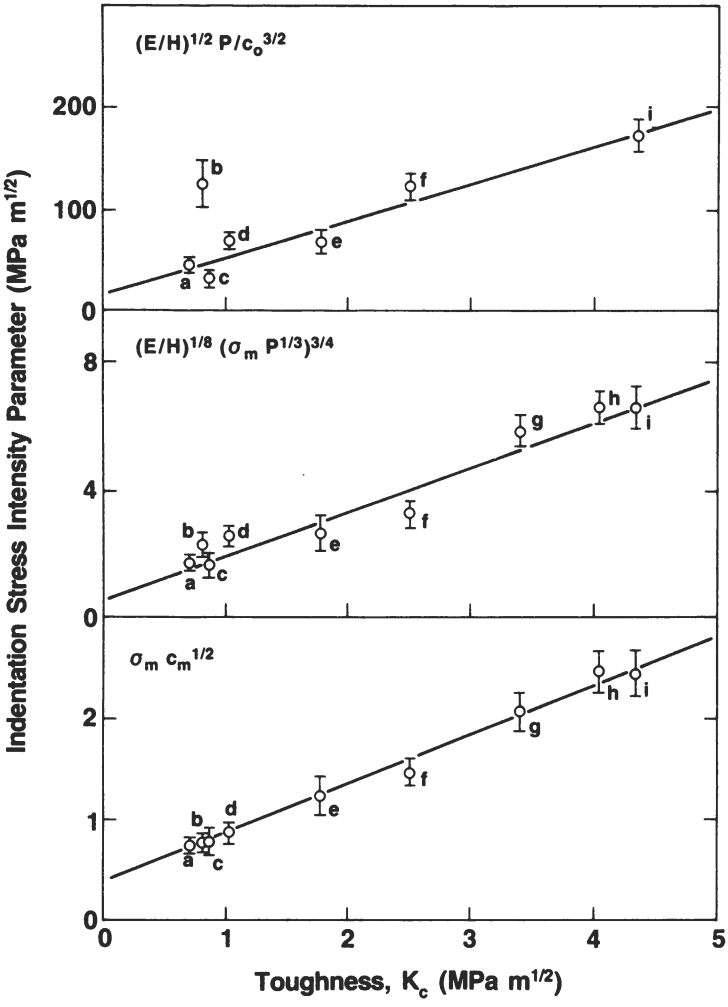

FIG. 7—*Plots of indentation test results illustrating the three toughness formulas, Eqs 10, 11, 12, for selected glasses and ceramics:* (a) *soda lime glass,* (b) *fused silica,* (c) *lead zirconium titanate,* (d) *barium titanate,* (e) *Synroc,* (f) *glass ceramic,* (g) *alumina I,* (h) *silicon carbide, and* (i) *alumina II. The vertical axis represents the measured indentation test variables; the horizontal axis represents the independently determined toughness values. The curves are linear fits to data.*

origins as required by Eqs 10 through 12. There is the implication here that some material dependence exists in the "proportionality constants" ξ, η, and ψ. The plots, nevertheless, remain useful representations for toughness calibration. It may be noted that the data points for some of the materials, especially fused silica (a material which, it will be recalled, deforms by densification), show significant departures from the line fits to the overall data in all but the third plot, reinforcing our previous allusion to Eq 12 as the most universal of the three toughness formulas.

Brittleness

The question often arises as to how one may quantify the "brittleness" of materials. Intuitively, brittleness should be a measure of the competition between deformation and fracture processes, as manifested, for instance, in the ductile-brittle transitions observed in structural metals. This competition has proved extremely difficult to formulate as a function of easily determinable material parameters. Here we shall propose that the ratio of hardness to toughness, H/K_c, be used as an appropriate index of brittleness (analogous to the adoption of H/E as an index of rigidity) [*33*]. Then the way is open, through Eq 8, to evaluate the relative susceptibilities to flow and fracture in terms of indentation threshold conditions.

To illustrate, let us consider the plot of the experimentally measured threshold indent size, a_c, as a function of $(E/H)(K_c/H)^2$ in Fig. 8 [*34*,*35*].

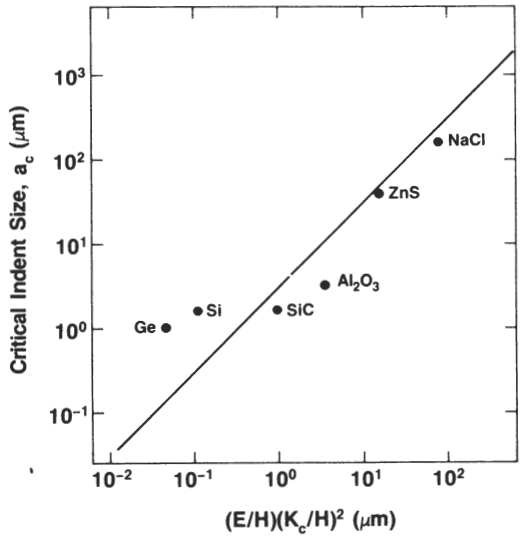

FIG. 8—*Plot of the measured threshold indentation size against* $(E/H)(K_c/H)^2$ *for selected ceramic materials. The line is best fit to Eq 8.*

Points to the lower left of this plot represent materials for which cracking is most easily produced at local stress concentrations, that is, which are relatively brittle. Conversely, the upper right of the plot represents the domain of more ductile materials, notably metals. In this interpretation, brittleness is quantified as a size effect. Physically, a_c represents the scale of damage above which the mechanical response is essentially fracture dominated and below which it is essentially deformation dominated.

The utility of this interpretation is most evident in the description of surface removal processes. If a surface is contacted with coarse particles, material removal occurs by a chipping mode (grinding), and if with fine particles, by a flow mode (polishing). The critical particle size defining the transition between these two modes is then dependent on the index H/K_c.

Surface Stress Evaluation

The surfaces of materials can undergo treatments which differ from those experienced by the underlying bulk and can thereby be left in a state of residual stress. Such stresses, although often confined to very shallow layers, can be of high intensities and can therefore exert a strong influence on mechanical properties. Indentation crack patterns can be used in brittle materials to evaluate these stresses. Basically, the surface traces of the radial crack system expand or contract, depending on whether the stresses are tensile or compressive. Figure 9, which shows Vickers indentations at the same load in annealed (stress-free) and thermally tempered (residual-compression) soda lime glass, illustrates the effect [*19*]. The fracture mechanics formulation then allows us, through appropriate modifications of the previous stress intensity relations, to establish a quantitative base for analysis.

Calculation of the surface stress is relatively straightforward when the stress is uniformly distributed over the prospective indentation crack area. We can then define a stress intensity factor conjugate to the surface stress, σ_s, $K_s = \psi\sigma_s c^{1/2}$, in the manner that K_a was defined earlier for substitution into Eq 6. Thus, in combination with Eq 4, one can solve to obtain a simple working expression for evaluating σ_s in terms of direct crack-size measurements, c. Alternatively, in a controlled-flaw test we may retain Eq 6 as our starting expression for calculating strengths, provided we replace σ_a by $\sigma_a + \sigma_s$. Accordingly, using the same logical development as in the derivation of Eq 7, we can readily show that, for a fixed indentation load, the critical applied stress at failure instability is given simply by

$$\sigma_m = \sigma_m^0 - \sigma_s \tag{13}$$

where σ_m^0 now refers to surfaces in the stress-free state. Two sets of strength tests, one on the actual surface-stressed materials and the other on stress-free controls, should then suffice to determine σ_s. Figure 10 shows the strength

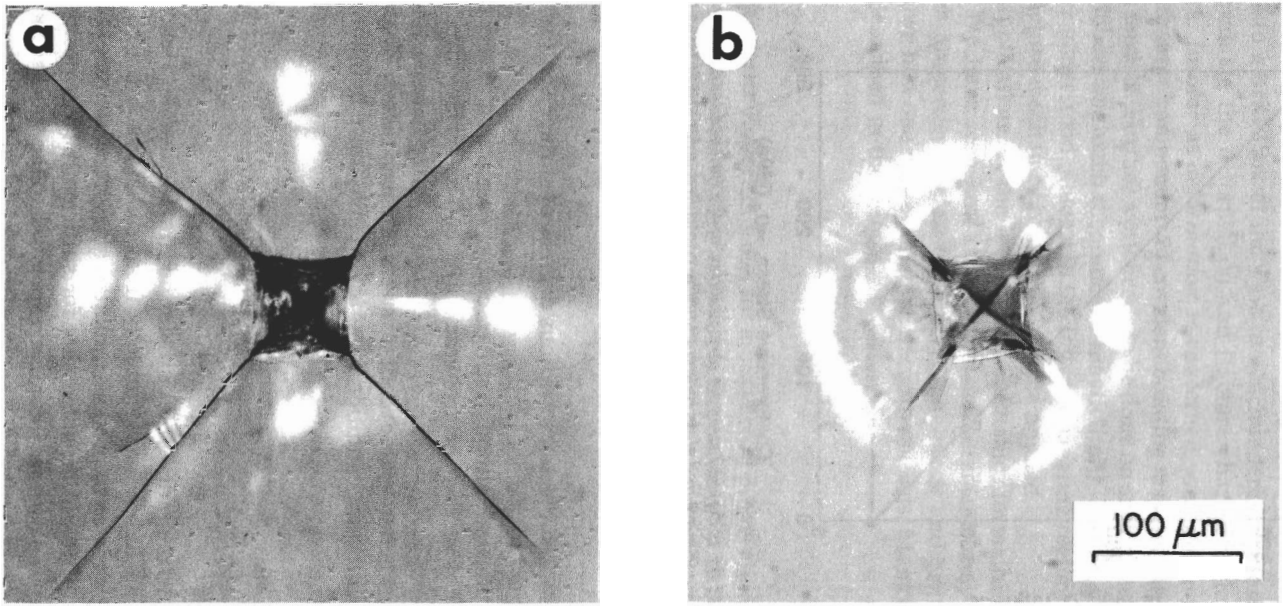

FIG. 9—*Vickers crack patterns in* (a) *preannealed and* (b) *thermally tempered soda lime glass. The indentation load was the same in both cases. Surface stresses in the tempered specimen have clearly inhibited the crack expansion.*

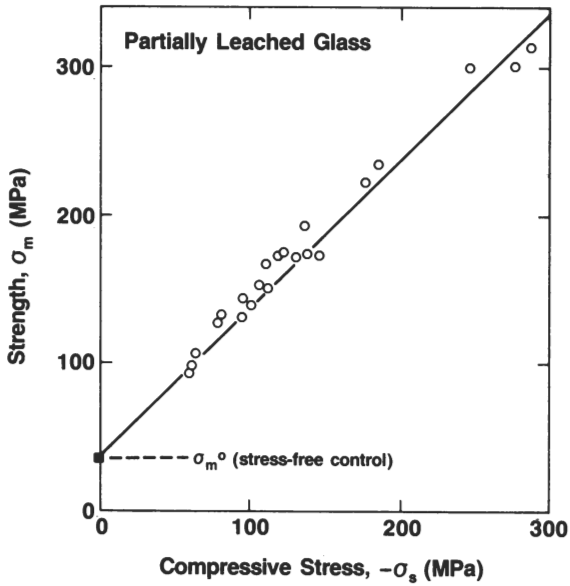

FIG. 10—*Plot of the measured strength as a function of the independently determined compression stress for surface-treated glass rods containing controlled indentation flaws (indentation load = 100* N*).*

data for glass rods subjected to various degrees of surface compression by a "partial leaching" treatment [*36*].

A more complicated, although still tractable, case is that of very thin stress layers, of depth $d \ll$ prospective crack size, c. The surface stress intensity factor in this limit is $K_s = 2\psi\sigma_s d^{1/2}$ [*37*]. In the immediate postindentation state, K_s augments the residual contact stress intensity factor, K_r, in Eq 4, so that, at the equilibrium condition $K = K_c$, we may solve to obtain [*37*]

$$\frac{c}{c^0} = \frac{1}{(1 - 2\psi\sigma_s d^{1/2}/K_c)^{2/3}} \tag{14}$$

where c^0 refers to the radial crack size in the stress-free state. Hence, the surface stresses can be evaluated directly from radial crack length measurements. Tensile stresses in proton-irradiated glass have been measured using this formulation. It will be noted that for sufficiently large positive σ_s, c is predicted to expand without limit, corresponding to the spontaneous fracture of the surface stress layer. Such surface breakup is, indeed, observed in the irradiated glass specimens [*37*].

Conclusions

We have had a brief look at the ways in which indentation testing may be applied to evaluate the deformation and fracture characteristics of glasses and ceramics. Insofar as *deformation* is concerned, we have indicated that materials with large components of covalent bonding may not satisfy the classic plasticity models. Further work needs to be done on such materials, whose hardness numbers approach theoretical strength limits. The *fracture* properties are better understood, at least in the fully propagating region, where conventional fracture mechanics principles may be applied.

Selective applications of the indentation mechanics formalism have been considered. We have seen how indentation measurements may be used to quantify such properties as elastic recovery, toughness, and brittleness. We have also shown how one may evaluate surface stress levels. Many other applications are described in the references.

Acknowledgments

The authors thank Robert F. Cook for assistance in preparation of data for some of the figures. This work was funded, in part, by the U.S. Air Force Office of Scientific Research and the U.S. Office of Naval Research.

References

[1] Lawn, B. R. and Wilshaw, T. R., *Fracture of Brittle Solids*, Cambridge University Press, London, 1975.

[2] Lawn, B. R. and Wilshaw, T. R., *Journal of Materials Science*, Vol. 10, 1975, pp. 1049–1081.

[3] Evans, A. G. and Wilshaw, T. R., *Acta Metallurgica*, Vol. 24, 1976, pp. 939–956.

[4] Lawn, B. R. in *Fracture Mechanics of Ceramics*, Vol. 5, R. C. Bradt, A. G. Evans, D. P. H. Hasselman, and F. F. Lange, Eds., Plenum, New York, 1983, pp. 1–25.

[5] Lawn, B. R. and Wiederhorn, S. M. in *Contact Mechanics and Wear of Rail/Wheel Systems*, J. Kalousek, R. V. Dukkipati, and G. M. Gladwell, Eds., University of Waterloo Press, Vancouver, 1983, pp. 133–148.

[6] Lawn, B. R., Hockey, B. J., and Richter, H., *Journal of Microscopy*, Vol. 130, 1983, pp. 295–308.

[7] Lawn, B. R. in *Strength of Glass*, C. R. Kurkjian, Ed., Plenum, New York, in press.

[8] Tabor, D., *The Hardness of Metals*, Clarendon, Oxford, 1951.

[9] Samuels, L. E. and Mulhearn, T. O., *Journal of Mechanics and Physics of Solids*, Vol. 5, 1957, pp. 125–134.

[10] Marsh, D. M., *Proceedings of the Royal Society of London*, Vol. A279, 1964, pp. 420–435.

[11] Hill, R., *The Mathematical Theory of Plasticity*, Oxford University Press, London, 1950, Chapter 5, pp. 97–105.

[12] Hagan, J. T. and Swain, M. V., *Journal of Physics D: Applied Physics*, Vol. 11, 1978, pp. 2091–2102.

[13] Ernsberger, F. M., *Journal of the American Ceramic Society*, Vol. 51, 1968, pp. 545–547.

[14] Arora, A., Marshall, D. B., Lawn, B. R., and Swain, M. V., *Journal of Non-Crystalline Solids*, Vol. 31, 1979, pp. 415–428.

[15] Multhopp, H., Lawn, B. R., and Dabbs, T. P. in *Plastic Deformation of Plastic Materials*, R. E. Tressler and R. C. Bradt, Eds., Plenum, New York, 1984, p. 681.

[16] Lawn, B. R. and Marshall, D. B. in *Fractography of Glass*, R. C. Bradt and R. E. Tressler, Eds., Plenum, New York, in press.
[17] Lawn, B. R., Dabbs, T. P., and Fairbanks, C. J., *Journal of Materials Science*, Vol. 18, 1983, pp. 2785-2797.
[18] Dabbs, T. P., Marshall, D. B., and Lawn, B. R., *Journal of the American Ceramic Society*, Vol. 63, 1980, pp. 224-225.
[19] Marshall, D. B. and Lawn, B. R., *Journal of Materials Science*, Vol. 14, 1979, pp. 2001-2012.
[20] Lawn, B. R. and Howes, T. R., *Journal of Materials Science*, Vol. 16, 1981, pp. 2745-2752.
[21] Marshall, D. B., Noma, T., and Evans, A. G., *Journal of the American Ceramic Society*, Vol. 65, 1982, pp. C175-C176.
[22] Loubet, J. L., Georges, J. M., and Meille, G., in this publication, pp. 72-89.
[23] Lawn, B. R., Evans, A. G., and Marshall, D. B., *Journal of the American Ceramic Society*, Vol. 63, 1980, pp. 574-581.
[24] Marshall, D. B., Lawn, B. R., and Evans, A. G., *Journal of the American Ceramic Society*, Vol. 65, 1982, pp. 561-566.
[25] Marshall, D. B., Lawn, B. R., and Chantikul, P., *Journal of Materials Science*, Vol. 14, 1979, pp. 2225-2235.
[26] Lawn, B. R. and Evans, A. G., *Journal of Materials Science*, Vol. 12, 1977, pp. 2195-2199.
[27] Hagan, J. T., *Journal of Materials Science*, Vol. 14, 1979, pp. 2975-2980.
[28] Palmqvist, S., *Archiv für das Eisenhuettenwesen*, Vol. 33, 1962, pp. 629-633.
[29] Anstis, G. R., Chantikul, P., Lawn, B. R., and Marshall, D. B., *Journal of the American Ceramic Society*, Vol. 64, 1981, pp. 533-538.
[30] Chantikul, P., Anstis, G. R., Lawn, B. R., and Marshall, D. B., *Journal of the American Ceramic Society*, Vol. 64, 1981, pp. 539-543.
[31] Cook, R. F. and Lawn, B. R., *Journal of the American Ceramic Society*, Vol. 66, 1983, pp. C200-C201.
[32] Cook, R. F., Lawn, B. R., and Anstis, G. R., *Journal of Materials Science*, Vol. 17, 1982, pp. 1108-1116.
[33] Lawn, B. R. and Marshall, D. B., *Journal of the American Ceramic Society*, Vol. 62, 1979, pp. 347-350.
[34] Lankford, J. and Davidson, D. L., *Journal of Materials Science*, Vol. 14, 1979, pp. 1662-1668.
[35] Chiang, S. S., Marshall, D. B., and Evans, A. G., *Journal of Applied Physics*, Vol. 53, 1982, pp. 312-317.
[36] Chantikul, P., Marshall, D. B., Lawn, B. R., and Drexhage, M. G., *Journal of the American Ceramic Society*, Vol. 62, 1979, pp. 551-555.
[37] Lawn, B. R. and Fuller, E. R., *Journal of Materials Science*, Vol. 19, 1984, p. 4061.

DISCUSSION

P. Sargent[1] *(written discussion)*—The analysis presented in this paper is based on the principle that as far as the growing cracks are concerned, there is no plasticity at the crack tip. However, the hardness value (which depends on the plasticity of the material) does enter the formulas because it is related to the magnitude of the stresses around the indentation. The effects of indentation size on hardness values are quite marked, especially for hard and brit-

[1]Department of Engineering, University of Cambridge, Cambridge CB2 1PZ, England.

tle materials. Have you thought of including some kind of indentation size effect correction in your data analysis or theory?

D. B. Marshall and B. R. Lawn (authors' closure)—The indentation hardness becomes size dependent only at small indentation diameters, typically $\lesssim 10$ μm for brittle materials. This size range generally falls within the subthreshold region, in which well-developed cracks do not form. Thus, the hardness/indentation-size effect may affect the critical threshold condition (for example, Eq 8). However, at larger indentation sizes, corresponding to well-developed fracture, the hardness is essentially independent of size.